Collective behavior in globally coupled systems consisting of two kinds of competing cells

Y. Zhang,[1,*] G. Hu,[2,1] H. Liu,[1] and J. H. Xiao[3]
[1]*Physics Department, Beijing Normal University, Beijing 100875, China*
[2]*Center for Advanced Science and Technology, CCAST (World Laboratory), Beijing 8730, China*
[3]*Department of Basic Science, Beijing University of Posts and Telecommunications, Beijing 100088, China*
(Received 11 August 1997)

We investigate a model of globally coupled systems consisting of two kinds of competing cells subject to stochastic forcings. The problem of large numbers of coupled Langevin equations can be reduced to a simple problem of two-dimensional differential equations. The global variables of the system show three types of collective phases: disordered phase, ordered steady phase, and coherent oscillation phase, and the transition conditions between these phases can be accurately predicted in the thermodynamic limit. A stochastic resonancelike behavior in the coherent oscillation output is revealed, and numerical simulations confirm the analytical results satisfactorily. [S1063-651X(98)07001-9]

PACS number(s): 05.40.+j

I. INTRODUCTION

The problem of coupled nonlinear systems has attracted considerable interest in the past decades, which study has uncovered a variety of collective behaviors [1–4], such as chorusing crickets, networks of neurons and synchronization transition in Josephson series arrays, etc. In the past decade, a large number of studies on this aspect have been related to noise-driven problems, where the topics of noise-induced phase transitions and stochastic resonance (SR) demonstrated around these phase transitions have become most active [5–15] (for the latest review, see [15]). It has been shown that the SR effect of global variables (or say macroscopic variables) can be induced by the mutual actions of noise, coupling, and external periodical forcing, among which the external periodic force is the critical ingredient for the SR behavior of spatiotemporal systems [6–8,12,14,15].

As yet, no clear advancement has been seen in the collective SR effect and other collective effects for coupled systems without an external signal. Knowledge in this respect is extremely important. On one hand, coupled autonomous systems exist in nature very popularly, therefore a deep understanding of the characteristic features of these systems must be of practical interest. On the other hand, the understanding of the dynamics of the basic autonomous systems can certainly help us to thoroughly analyze the response behavior of the systems to external forces.

In Sec. II, we describe our model of noise-driven globally coupled systems with two kinds of competing cells, and reduce the high-dimensional Langevin equations to two coupled ordinary differential equations in a large system size limit (the so-called thermodynamic limit). Three kinds of phase transitions are revealed. In Sec. III, we investigate the synchronized oscillation of the macroscopic output, and find stochastic resonance in this synchronization process. For finite cell number, we modify the two coupled ordinary differential equations to two coupled Langevin equations to take into account the fluctuation caused by finite system size effect. The numerical results of direct simulations of the high-dimensional Langevin equations coincide with those of the much simplified two-dimensional system satisfactorily, and then the validity of our theoretical analysis is well confirmed.

II. MODEL AND PHASE TRANSITION DIAGRAM

In the present work, we are interested in the collective phases and the possibility of the collective SR without external signal in coupled noisy bistable systems. Similar to Ref. [8], we consider a model of globally coupled two-series cells which are indicated by (x_i, y_i), $i=1,2,...,N$. The inner dynamics of each cell is described by

$$\dot{x} = ax - x^3 + \Gamma(t),$$
$$\dot{y} = y - y^3 + \Delta(t), \tag{2.1}$$

where $a>0$. While all cells are globally coupled to each other through a single quantity $Z=X-Y$, $X=(1/N)\Sigma_{i=1}^{i=N} x_i$, $Y=(1/N)\Sigma_{j=1}^{j=N} y_j$, x is regarded as being active, and y is suppressive. The competition between x and y yields many interesting features of this model. The idea of the competition between activators and suppressors appears in many fields. Then, our model can be formulated as

$$\dot{x}_i = ax_i - x_i^3 + \mu_1 Z(t) + \Gamma_i(t),$$
$$\dot{y}_j = y_j - y_j^3 + \mu_2 Z(t) + \Delta_i(t),$$
$$\langle \Gamma_i(t) \rangle = 0, \quad \langle \Gamma_i(t)\Gamma_{i'}(t') \rangle = 2D_1 \delta_{ii'} \delta(t-t'),$$
$$\langle \Delta_j(t) \rangle = 0, \quad \langle \Delta_j(t)\Delta_{j'}(t') \rangle = 2D_2 \delta_{jj'} \delta(t-t'),$$
$$\langle \Gamma_i(t)\Delta_j(t') \rangle = 0, \tag{2.2}$$

where we take $a=0.9$, $\mu_2=\beta\mu_1$, and $D_1=D_2=D$ throughout the paper. In all of the following, we investigate the macroscopic state in phase space (X,Y), which shows the collective behavior of the microscopic variables $(x_1, y_1; \ldots; x_N, y_N)$. The positive couplings in Eqs. (2.2) can also be regarded as the diffusive couplings, and the negative

*Author to whom correspondence should be addressed.

ones as the resistancelike couplings. It is interesting to investigate the effect caused by their interaction. Our analysis is based on the conditions

$$\mu_{1,2},\ D \ll 1 \quad \text{and} \quad N \gg 1. \tag{2.3}$$

The inequality $\mu_{1,2} \ll 1$ guarantees bistability of each x_i and y_j in the system (2.2). It will be shown that the analytical results can be well confirmed by numerically running the original spatiotemporal stochastic systems (2.2) at small while finite D, $\mu_{1,2}$, and large while finite N.

Under the condition (2.3), the continuous bistable systems Eqs. (2.2) can be reduced to two-state ones for x_i and y_j, respectively, and then the coupled stochastic bistable systems can be simplified to the following coupled master equations [6]:

$$\dot{P}^{\pm}_{x_i} = -R_x P^{\pm}_{x_i} + R^{\mp}_x, \quad P^{+}_{x_i} + P^{-}_{x_i} = 1, \quad i = 1,2,...,N,$$

$$\dot{P}^{\pm}_{y_j} = -R_y P^{\pm}_{y_j} + R^{\mp}_y, \quad P^{+}_{y_j} + P^{-}_{y_j} = 1, \quad j = 1,2,...,N, \tag{2.4}$$

where $P^{+}_{x_i}$ and $P^{-}_{x_i}$ ($P^{+}_{y_j}$ and $P^{-}_{y_j}$) are the probabilities for x_i (y_j) to take the state $+\sqrt{a}$ and $-\sqrt{a}$ ($+1$ and -1), respectively; R^{+}_x (R^{-}_x) is the transition rate from state $+\sqrt{a}$ to $-\sqrt{a}$ ($-\sqrt{a}$ to $+\sqrt{a}$) for x, and R^{+}_y (R^{-}_y) is that from $+1$ to -1 (-1 to $+1$) for y, respectively, which reads

$$R^{\pm}_x = \frac{a}{\sqrt{2}\pi} \exp\left(-\frac{a^2}{4D} \mp \frac{\sqrt{a}\mu_1 Z}{D} \right), \quad R_x = R^{+}_x + R^{-}_x$$

$$= r_{01} \cosh\left(\frac{\sqrt{a}\mu_1 Z}{D} \right),$$

$$R^{\pm}_y = \frac{1}{\sqrt{2}\pi} \exp\left(-\frac{1}{4D} \mp \frac{\mu_2 Z}{D} \right), \quad R_y = R^{+}_y + R^{-}_y$$

$$= r_{02} \cosh\left(\frac{\mu_2 Z}{D} \right),$$

$$r_{01} = \frac{a\sqrt{2}}{\pi} \exp\left(-\frac{a^2}{4D} \right), \quad r_{02} = \frac{\sqrt{2}}{\pi} \exp\left(-\frac{1}{4D} \right). \tag{2.5}$$

By averaging Eqs. (2.4),

$$\langle X(t) \rangle = \frac{1}{N} \sum_{i=1}^{N} [\sqrt{a} P^{+}_{x_i} + (-\sqrt{a}) P^{-}_{x_i}],$$

$$\langle Y(t) \rangle = \frac{1}{N} \sum_{j=1}^{N} [P^{+}_{y_j} + (-1) P^{-}_{y_j}], \tag{2.6}$$

we can further reduce the N coupled master equations to two-dimensional differential equations

$$\langle \dot{X}(t) \rangle = -r_{01} \cosh\left(\frac{\sqrt{a}\mu_1 Z}{D} \right) \langle X(t) \rangle + \sqrt{a} r_{01} \sinh\left(\frac{\sqrt{a}\mu_1 Z}{D} \right), \tag{2.7}$$

$$\langle \dot{Y}(t) \rangle = -r_{02} \cosh\left(\frac{\mu_2 Z}{D} \right) \langle Y(t) \rangle + r_{02} \sinh\left(\frac{\mu_2 Z}{D} \right).$$

In the thermodynamic limit $N \to \infty$, $X(t) = \langle X(t) \rangle$ and $Y(t) = \langle Y(t) \rangle$; then we have

$$\dot{X}(t) = -r_{01} \cosh\left(\frac{\sqrt{a}\mu_1 Z}{D} \right) X(t) + \sqrt{a} r_{01} \sinh\left(\frac{\sqrt{a}\mu_1 Z}{D} \right),$$

$$\dot{Y}(t) = -r_{02} \cosh\left(\frac{\mu_2 Z}{D} \right) Y(t) + r_{02} \sinh\left(\frac{\mu_2 Z}{D} \right). \tag{2.8}$$

The stationary solution of Eqs. (2.8) can be worked out as

$$Z = \sqrt{a} \tanh\left(\frac{\sqrt{a}\mu_1 Z}{D} \right) - \tanh\left(\frac{\beta\mu_1 Z}{D} \right). \tag{2.9}$$

It is clear that $Z = 0$ is always a solution of Eq. (2.9), i.e., $X = Y = 0$ is always a stationary solution of Eqs. (2.8). Stability analysis of $X = Y = 0$ shows that this solution may lose its stability in two cases,

$$\mu_1 (r_{02}\beta - r_{01} a) + (r_{01} + r_{02}) D \geqslant 0 \tag{2.10a}$$

and

$$\mu_1 (a - \beta) \geqslant D. \tag{2.10b}$$

In the former case [i.e., by changing the left side of (2.10a) from <0 to >0], the solution $X = Y = 0$ changes from a stable focus to an unstable focus, i.e., it undergoes a Hopf bifurcation; in the latter case [changing $\mu_1(a-\beta)$ from $<D$ to $>D$] the origin changes from a stable node to a saddle, i.e., it undergoes a saddle-node bifurcation. Thus, we presume the system may have three phases: the stable state $X = Y = 0$ (corresponding to disordered phase), the bistable state (corresponding to spontaneous ordering phase), and the coherent oscillation state (corresponding to the spontaneous spatiotemporal synchronization moving phase), which are actually found and plotted in Fig. 1, where the dashed and solid lines are drawn by Eqs. (2.10a) and (2.10b), respectively. As $\mu_1 \mu_2 > 0$, we can observe all three phases, while as $\mu_1 \mu_2 < 0$, the coherent oscillation phase can never occur, and only the first two phases can be observed. Two interesting points in these figures are worth noting. First, codimension-2 bifurcation can be identified at the intersections of the saddle node and Hopf bifurcation critical curves, in the vicinity of which some interesting and complicated dynamics may be expected. Second, the two phases of the bistable state and coherent oscillation are separated by global heteroclinic bifurcation [disked lines in Fig. 1(a)]; this bifurcation condition cannot be given explicitly. The disks are obtained by numerical simulations on Eqs. (2.8). Further investigation shows that no bistable state exists for $\beta > a$ and $\mu_1 > 0$, and this agrees with the results in Ref. [8], where we took $\beta = a$, $\mu_1 > 0$ and could find the disordered and coherent oscillation phases only (no bistable ordered phase exists).

Figure 2(a) plots out the schematic phase diagram by fixing $\mu_1 = 0.08$, where the regions 1,2,3 represent the stable $X = Y = 0$ solution, the bistable state, and coherent oscillation, respectively. Figure 2(b) shows the detailed behavior of

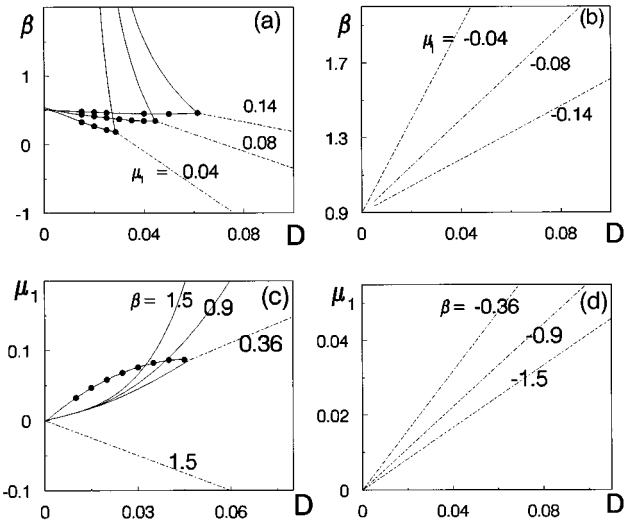

FIG. 1. The boundaries separating various phases of the state of Eqs. (2.8). The dashed and solid lines indicate pitchfork and Hopf bifurcations from stable $X=Y=0$ to bistable and synchronized oscillation states, respectively. $X=Y=0$ is stable on the right side of these two critical lines. The disked lines represent the critical parameters separating two regions of bistability and coherent oscillation. (a) $\mu_1>0$, $\mu_1=0.04,0.08,0.14$; (b) $\mu_1<0$, $\mu_1=-0.04$, $-0.08,-0.14$; (c) $\beta>0$, $\beta=0.36,0.90,1.25$; (d) $\beta<0$, $\beta=-0.36$, $-0.9,-1.25$.

the system as the noise intensity increases for the coupling $\mu_1=0.08$ and $\beta=0.36$ [along the horizontal dotted line in Fig. 2(a)]. The results are obtained by simulating Eqs. (2.8) with the four-step Runge-Kutta procedure, in which at least 20 000 relaxation steps are eliminated. All sites are located in the four wells $(\pm\sqrt{a},\pm 1)$. The competition between coupling and noise determines the balance of the population occupations in these four wells, and then determines the value of the global variable $Z=X-Y$. The system shows the bistable phase for small D. By increasing D to cross the heteroclinic bifurcation line, we can find the limit cycle solution, after which the spatially synchronized and temporally periodic oscillation phase comes into being. By increasing D further, the amplitude of the limit cycle decreases, and finally shrinks to the stable fixed point $X=Y=0$ (stable focus) via the inverse Hopf bifurcation.

Similar to Fig. 2(b), Fig. 2(c) shows the detailed behavior along the vertical dotted line in Fig. 2(a), on which we fix $\mu_1=0.08$ and $D=0.04$ and have β increased from $\beta=-1$ to 1. In the case of $\beta<-1$ all cells are drawn into the state $(\sqrt{a},-1)$ or the state $(-\sqrt{a},+1)$; that produces the macroscopic variable $Z=X-Y\approx\pm(1+\sqrt{a})$. The amplitude of Z can be reduced by increasing β due to the balance of the population occupations in the four wells $(\pm\sqrt{a},\pm 1)$. By further increasing β, we find both heteroclinic bifurcation to the limit cycle solution and inverse Hopf-bifurcation to a unique stable steady solution $X=Y=0$; this is again consistent with the phase figure of Fig. 2(a).

III. STOCHASTIC RESONANCE IN THE SYNCHRONIZED COHERENT OUTPUT, FINITE SIZE EFFECT

From Fig. 2(b), it is clear that no coherent oscillation can be found for either very small or very large D; intense collective oscillation can be observed only in a certain intermediate range of D. Therefore, there must exist a value of D in which the optimum matching of coupling and noise exerts the strongest spatiotemporal synchronization. Too weak noise is not able to stimulate oscillation, while too strong noise may destroy coherent motion. It is easy to accept that the optimum collective synchronization only occurs when the noise intensity and the coupling density are comparable.

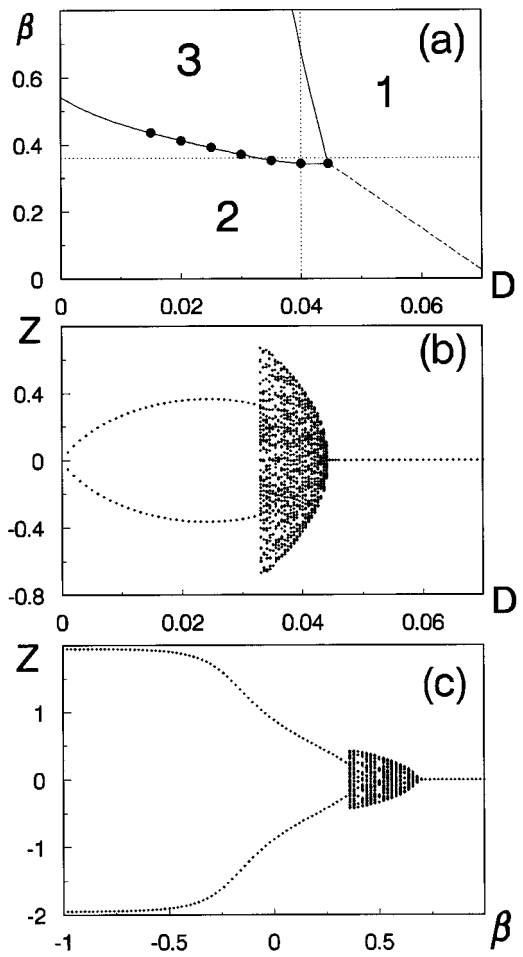

FIG. 2. (a) Schematic phase diagram of global variable Z in $\beta-D$ plane. $\mu_1=0.08$ and all curves have the same meanings as Fig. 1. Regions 1, 2, and 3 represent disordered state $X=Y=0$, bistable state for steady nonzero X and Y, and synchronized oscillation, respectively. The intersection of dashed, solid, and disked curves is a codimension-2 bifurcation point. (b) Asymptotic bifurcation diagram of Z versus noise intensity D. $\beta=0.36$. [The horizontal line of (a)]. (c) Asymptotic bifurcation diagram of Z versus coupling parameter β. $D=0.04$ [the vertical line of (a)].

For quantitatively measuring the intensity of the output coherent motion, we quote the classical dimensionless kinetic energy

$$E_k=\lim_{T\to\infty}\frac{1}{T}\int_0^T\left[\frac{1}{2}\left(\frac{dX(t)}{dt}\right)^2+\frac{1}{2}\left(\frac{dY(t)}{dt}\right)^2\right]dt. \quad (3.1)$$

Since $E_k=0$ corresponds to static output, while large E_k shows strong synchronized oscillation, it is reasonable to use E_k to measure the noise-induced coherence. Figure 3 takes parameter values the same as Fig. 2(b), and we plot E_k vs D,

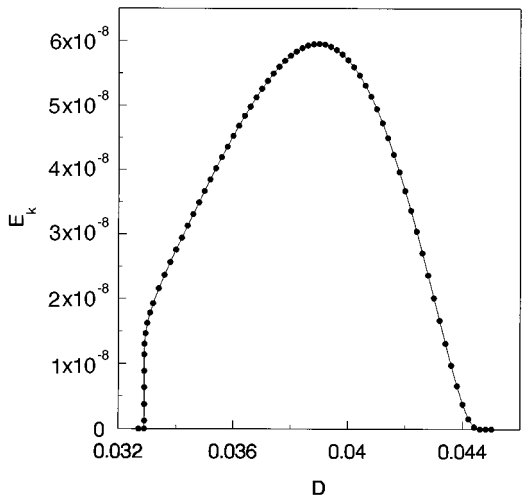

FIG. 3. The dimensionless kinetic energy vs noise intensity D. E_k is computed from Eqs. (2.8) and (3.1), along with the horizontal line in Fig. 2(a).

where a resonancelike response peak is obviously observed; this is reminiscent of a SR since the resonance is purely noise-induced, and the peaked curve is shown against noise intensity.

All the results from Fig. 1 to Fig. 3 are obtained from Eqs. (2.8), which are derived for the limit $N\to\infty$. Practically, we are dealing with large while finite N. Therefore, $X(t)$ and $Y(t)$ should be subject to certain fluctuations. To take into account the finite size effect and improve our derivation, we start from Eqs. (2.7), and replace the identities $X(t)=\langle X(t)\rangle$ and $Y(t)=\langle Y(t)\rangle$ by

$$X(t)=\langle X(t)\rangle+\eta(t),$$

$$Y(t)=\langle Y(t)\rangle+\xi(t). \tag{3.2}$$

For large while finite N, the statistical property of $\eta(t)$ and $\xi(t)$ can be computed, based on the assumption that the variations of the macroscopic variables $X(t)$ and $Y(t)$ are much slower than the variations of the microscopic variables $x_{i=}\sqrt{a}(P^+_{x_i}-P^-_{x_i})$ and $y_j=P^+_{y_j}-P^-_{y_j}$, and then we can consider $X(t)$ and $Y(t)$ to be constant when we compute the variances of x_i and y_j (the so-called adiabatic approximation treatment). A direct computation with Eqs. (2.4) gives

$$\langle\eta(t)\eta(t')\rangle=\frac{1}{N^2}\sum_{i=1}^{i=N}\langle\Delta x_i(t)\Delta x_i(t')\rangle$$

$$=\frac{a}{N\cosh^2\left[\frac{\sqrt{a}\mu_1 Z}{D}\right]}\exp(-R_x|t-t'|), \tag{3.3}$$

$$\langle\xi(t)\xi(t')\rangle=\frac{1}{N^2}\sum_{j=1}^{j=N}\langle\Delta y_j(t)\Delta y_j(t')\rangle$$

$$=\frac{1}{N\cosh^2\left[\frac{\mu_2 Z}{D}\right]}\exp(-R_y|t-t'|),$$

$$\langle\eta(t)\xi(t')\rangle=\langle\xi(t)\eta(t')\rangle=0,$$

$$\langle\eta(t)\rangle=\langle\xi(t)\rangle=0.$$

By inserting Eqs. (3.2) into Eqs. (2.7), we arrive at two coupled stochastic equations

$$\dot{X}(t)=-r_{01}\cosh\left(\frac{\sqrt{a}\mu_1 Z}{D}\right)X(t)+\sqrt{a}r_{01}\sinh\left(\frac{\sqrt{a}\mu_1 Z}{D}\right)+R_x\eta(t)+\frac{d\eta(t)}{dt},$$

$$\dot{Y}(t)=-r_{02}\cosh\left(\frac{\mu_2 Z}{D}\right)Y(t)+r_{02}\sinh\left(\frac{\mu_2 Z}{D}\right)+R_y\xi(t)+\frac{d\xi(t)}{dt}, \tag{3.4}$$

where $\eta(t)$ and $\xi(t)$ are the effective colored noises having zero mean and exponentially decay correlations given in Eqs. (3.3). By identifying [16–18]

$$\frac{d\eta(t)}{dt}=-R_x\eta(t)+R_x\Lambda(t),$$

$$\frac{d\xi(t)}{dt}=-R_y\xi(t)+R_y\Pi(t), \tag{3.5}$$

we can reduce Eqs. (3.4) to

$$\dot{X}(t)=-r_{01}\cosh\left(\frac{\sqrt{a}\mu_1 Z}{D}\right)X(t)+\sqrt{a}r_{01}\sinh\left(\frac{\sqrt{a}\mu_1 Z}{D}\right)+R_x\Lambda(t),$$

$$\dot{Y}(t)=-r_{02}\cosh\left(\frac{\mu_2 Z}{D}\right)Y(t)+r_{02}\sinh\left(\frac{\mu_2 Z}{D}\right)+R_y\Pi(t),$$

$$\langle\Lambda(t)\Lambda(t')\rangle=2D_1'\delta(t-t'),\quad D_1'=\frac{a}{NR_x\left[\cosh\left(\frac{\sqrt{a}\mu_1 Z}{D}\right)\right]^2},$$

$$\langle\Pi(t)\Pi(t')\rangle=2D_2'\delta(t-t'),\quad D_2'=\frac{1}{NR_y\left[\cosh\left(\frac{\mu_2 Z}{D}\right)\right]^2},$$

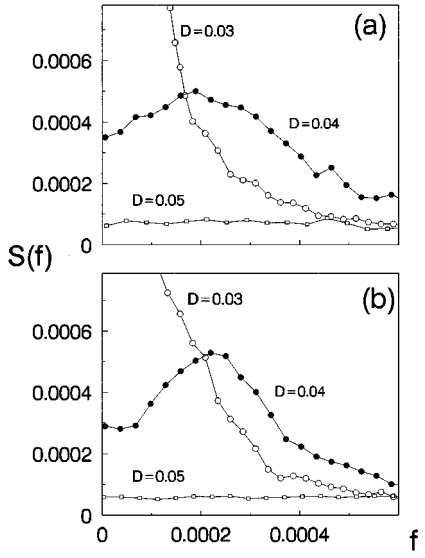

FIG. 4. The spectra of $X(t)$ for various D's. $N=100$, $\mu_1=0.08$, $\beta=0.36$. The best coherent output appears for intermediate D. (a) The results of Eqs. (2.2), (b) the results of Eqs. (3.6). Their results are very similar.

$$\langle \Lambda(t)\Pi(t')\rangle=\langle \Pi(t)\Lambda(t')\rangle=0, \quad \langle \Lambda(t)\rangle=\langle \Pi(t)\rangle=0. \tag{3.6}$$

Now the $2N$ ($\infty > N \gg 1$) coupled systems (2.2) or the $2N$ coupled master equations (2.4) are reduced to two coupled Langevin equations with white noises. This reduction is very general in the two-state approximation, irregardless of the particular form of the system. The statistical quantities of the noise are known explicitly. An interesting as well as desirable feature of Eqs. (3.6) is that we do not need to increase the dimension of the problem in order to treat the colored noises. Only white noises are retained in the equations after the cancellations; that greatly reduces the difficulty of the problem.

With noise, the quantity (3.1) is no longer adequate for measuring the coherence and the degree of the synchronization of the output, because fluctuation caused by noise can be accumulated in the integration. In order to better detect the intensity of the coherent output oscillation, we use the following quantity:

$$R=h(\Delta\omega/\omega_p)^{-1}, \tag{3.7}$$

where h is the highest height of the peak in the spectrum of $X(t)$, ω_p is the frequency at the peak center, and $\Delta\omega$ is the right half-width of the peak at the height $h_1=e^{-1/2}h$. In Ref. [19], the authors used this quantity to measure the degree of the output coherence of low-dimensional Langevin equations and regarded it as a signal-to-noise ratio (SNR) of a noisy autonomous system. In Fig. 4(a) we set $\mu_1=0.08$, $\mu_2=0.0288$, and $N=100$, and plot some spectra of $X(t)$ for different D by directly running Eqs. (2.2); the best coherent output appears for the intermediate D. In Fig. 4(b) we do the same as (a) by running the reduced Eqs. (3.6), and obtain very similar results. In Figs. 5(a) and 5(b), we compute R versus D by numerically running Eqs. (2.2) and (3.6), respectively. The parameters are taken as $N=100$, $\mu_1=0.08$, and $\beta=0.36$. From Fig. 5, two interesting points are noticed. First, we find a nice stochastic resonance response without external periodic forcing. There exists an optimal noise intensity for the given couplings at which the output contains the strongest coherent oscillation. This behavior is consistent with the behavior in Fig. 3. Second, the agreement between (a) and (b) is fairly good both qualitatively and quantitatively, although the system size N is not really large; this agreement confirms the validity of the above derivations from Eq. (2.2) to Eq. (3.6). Of course, the finite D, μ, and N still cause some visible deviations between Eqs. (2.2) and Eqs. (3.6) [i.e., between Figs. 4(a) and 4(b), and 5(a) and 5(b)]. Note, the computation of Eqs. (3.6) is incomparably less time consuming than that of the original $2N$-dimensional equations (2.2), thus this reduction is practically very useful.

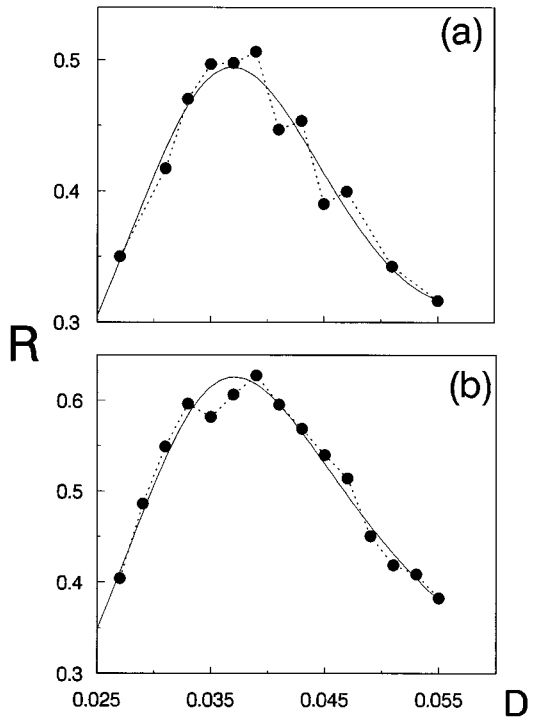

FIG. 5. The SNR (R) defined in Eq. (3.7) versus noise intensity D. $N=100$, $\mu_1=0.08$, and $\beta=0.36$. (a) The results of Eqs. (2.2). (b) The results of Eqs. (3.6). The agreement of both results is fairly good.

IV. CONCLUSION

In summary, this paper has investigated collective phases in globally coupled noise-driven systems with two competition series. In the thermodynamic limit and in the two-state approximation, we reduce the system of many coupled Langevin equations to enormously simpler two coupled ordinary differential equations, and find three different collective phases: the disordered phase $X=Y=0$; the ordered bistable phase, which can appear from the disordered phase via second-order pitch-fork bifurcation; and the coherent oscillation phase, which occurs from the disordered phase via Hopf bifurcation. There is a global heteroclinic bifurcation critical line separating the phases of bistability and oscillation. An interesting codimension-2 bifurcation point is iden-

tified at the intersection of all these three critical lines. It is emphasized that all these single- or multicodimensional phase transitions are purely noise induced.

Among all these three phases, we are most interested in noise-induced coherent oscillation. Two quantities, noise-induced kinetic energy and quality factor, are suggested to measure the noise-induced coherence and the degree of synchronization of the subsystems. With both quantities, interesting stochastic resonance for collective motion is found.

In large system size and small noise approximations, we reduce the original high-dimensional Langevin equations to two-dimensional Langevin equations. All the above characteristic features including fluctuation induced by finite system size can be well predicted by the reduced equations, and numerical simulations of the large systems confirm the validity of the analytical reduction.

ACKNOWLEDGMENTS

This work is supported by the National Natural Science Foundation of China, and Project of Nonlinear Science.

[1] A. T. Winfree, *The Geometry of Biological Time* (Springer, New York, 1980).
[2] S. H. Strogatz and I. Stewart, Sci. Am. **269**, 102 (1993).
[3] K. Wiesenfield, P. Colet, and S. H. Strogatz, Phys. Rev. Lett. **76**, 4043 (1996).
[4] H. A. Tanaka, A. J. Lichtenberg, and S. Oishi, Phys. Rev. Lett. **78**, 2140 (1997).
[5] M. Shiino, Phys. Rev. A **36**, 2393 (1987).
[6] P. Jung, U. Behn, E. Pantazelou, and F. Moss, Phys. Rev. A **46**, R1709 (1992).
[7] M. Morillo, J. G. Ordonez, and J. M. Casado, Phys. Rev. E **52**, 316 (1995).
[8] H. Gang, H. Haken, and X. Fagen, Phys. Rev. Lett. **77**, 1925 (1996).
[9] W. J. Rappel and A. Karma, Phys. Rev. Lett. **77**, 3256 (1997).
[10] X. Pei, L. Wilkens, and F. Moss, Phys. Rev. Lett. **77**, 4679 (1997).
[11] Proceedings of the NATO Advanced Research Workshop on Stochastic Resonance in Physics and Biology, edited by F. Moss, A. Bulsara, and M. Shlesinger [J. Stat. Phys. **70**, No. 1/2 (1993)].
[12] J. F. Lindner, B. K. Meadows, W. L. Ditto, M. E. Inchiosa, and A. R. Bulsara, Phys. Rev. Lett. **75**, 3 (1997).
[13] F. Marchesoni, L. Gammaitoni, and A. R. Bulsara, Phys. Rev. Lett. **76**, 1609 (1996).
[14] M. Locher, G. A. Johnson, and E. R. Hunt, Phys. Rev. Lett. **77**, 4698 (1996).
[15] L. Gammatoni, P. Hanggi, P. Jung, and F. Marchesoni, Rev. Mod. Phys. (to be published).
[16] P. Hanggi, F. Marchesoni, and P. Grigolini, Z. Phys. B **56**, 333 (1984).
[17] P. Jung and P. Hanggi, Phys. Rev. Lett. **61**, 11 (1988).
[18] G. P. Tsironis and P. Grigolini, Phys. Rev. A **78**, 3749 (1988).
[19] G. Hu, T. Ditzinger, C. Z. Ning, and H. Haken, Phys. Rev. Lett. **71**, 807 (1993).